Microwave Superdirectivity with Dimers of Helical Elements

P. Petrov,* A. P. Hibbins, and J. R. Sambles
Department of Physics and Astronomy, University of Exeter, Exeter EX4 4QL, United Kingdom

(Received 2 June 2019; revised manuscript received 17 March 2020; accepted 20 March 2020; published 6 April 2020)

Superdirective end-fire radiation in the low-GHz frequency range is demonstrated using magnetically coupled structures of subwavelength metallic helices. Numerical, experimental, and analytical results are presented on superdirective dimers that are almost 3 times smaller than those of previously demonstrated dimers of split-ring resonators (0.09λ compared with 0.25λ) and provide close to theoretical maximum values of directivity without using complex feeding networks. The size, directivity, efficiency, and operational passband width of such structures is optimized.

DOI: 10.1103/PhysRevApplied.13.044012

I. INTRODUCTION

The concept of superdirectivity was first proposed by Oseen almost a century ago [1]. He theoretically showed that a finite-size system could produce an arbitrarily narrow (i.e., directive) beam of radiation over a relatively small frequency band. Unlike conventional phased arrays that provide high directivity by means of constructive interference, the superdirective antennas are based on destructive interference. They suppress radiation in all directions, apart from the direction of the main lobe, where the destructive interference is a minimum, and hence, the radiation there is a relative maximum. This, in theory, makes it possible to obtain an arbitrarily narrow beam [2]. Further developments were undertaken by Uzkov [3], who demonstrated that an end-fire array, consisting of N isotropic elements, provided directivity tending to N^2 as the distance between the elements tended to zero. Directivity (D) here is defined as the power density radiated by the antenna in the direction of its strongest emission divided by the average power density radiated in all directions. Limitations on superdirectivity were demonstrated by Uzsoky and Solymar [4], who presented a mathematical procedure for finding the maximum directivity for a given array of radiating dipoles and calculated how the geometrical parameters of the structure could be optimized for the best directivity and gain.

As theoretically shown by Solymar [5], to attain the highest values of directivity, the fields in the system should exhibit strong spatial variations at distances shorter than the free-space wavelength. To achieve this, the amplitude and phase of the currents in each element of the array must be controlled precisely. However, this may be difficult to realize experimentally. An approach is suggested in Ref. [6] where the maximum possible directivity for two helices is achieved using a feeding network with a complex matching circuit to control the phase difference. Some other practical solutions have been suggested [7,8], but no general approach has been proposed to produce the required phase difference without feeding individual elements. For instance, the structure presented in Ref. [8] consists of four helical elements. Two geometries are presented with sizes of 0.65λ and 0.17λ, which produce directivity gains of 7.5 and 4.8 dBi, respectively. The performance of both structures appears to be far from the theoretical maximum suggested in Ref. [4] for the four-element superdirective array.

A fresh way to realize superdirectivity appeared with the emergence of metamaterials with studies on magnetoinductive (MI) waves [9,10], showing that coupling between the elements in an array can provide strong spatial variations of fields at distances shorter than the free-space wavelength. The first attempts to utilize arrays of resonant elements for superdirective antennas appear to be those of Buell *et al*. [11], who implemented metamaterial-based insulators to suppress parasitic coupling. Interelement coupling was first used to achieve optimal current distributions in the works of O'Donnell *et al.* [12,13]. They demonstrated a metamaterial-inspired parasitically coupled superdirective array antenna with just a single directly fed element, with all other elements shorted to a conductive ground plane. This research was continued by Lim and Ling [14], who proposed a two-element structure, with one of them fed and a second (one) passive with an overall size of 0.13λ that provided the realized gain of 6.19 dBi, with the gain dropping by 1 dB over a bandwidth of 2.82%. The presented structure consists of five specially designed helical-like wires (two acting as the driver and three as the reflector) that is a complex and hard to manufacture device.

In 2013, researchers proposed superdirective arrays with one element fed and the others left open [15,16]. It was predicted theoretically [4,17,18] that a far-field

*pp386@exeter.ac.uk

superdirectivity with a maximum value $D = 5.25 = 7.2$ dBi was possible in simple structures composed of two coupled split-ring resonators (SRRs), when the size and distance between them both tended to zero. The dipolelike radiation of neighboring elements can produce the destructive interference that is necessary for superdirectivity. The required phase difference between the currents in the resonators and their magnitudes provide strong negative magnetic coupling between them [19]. High values of D were shown for both MHz [19,20] and GHz [21] frequency ranges using dimers formed of two coplanar SRRs, with the first being driven and the second passively excited. It was theoretically demonstrated [15,21] that the directivity of such a structure depended on several parameters: the coupling coefficient, κ; the center-to-center distance, a; the operating wave number, k; and the quality factor, Q. To achieve the theoretical maximum value of directivity, the following relationship between them needs be satisfied:

$$\frac{Q|\kappa|}{\sqrt{1-\kappa/2}} = \alpha\frac{5}{\kappa a'}, \tag{1}$$

where α is a dimensionless parameter that depends on the geometry of the elements.

Other ways to use metamaterial-inspired structures for superdirective antennas can be found in Ref. [22], where low-profile monopoles are implemented, and in Ref. [23], where a superdirective horn antenna is designed.

Here, we propose an alternative element geometry: a metal helix in the normal mode of radiation. It demonstrates benefits in terms of both size reduction and improved directivity of the superdirective dimer structure, when compared with previous work using SRRs. This allows us to show that, when taking into account strong magnetic coupling between elements, a close to theoretical maximum value of directivity can be achieved using a simple two-element structure. The radiation properties of the helical dimer structures are analyzed for different frequencies and element configurations using numerical modeling, analytical calculations, and experimental measurements. In addition, we discuss ways for superdirective dimer optimization in terms of different antenna parameters, exploring the size of the structure, directivity, efficiency, and operational passband width.

II. DIMER GEOMETRIES

In previous studies, SRRs have been used to construct structures that exhibit superdirective radiation [20,24]. At high frequencies, the dimensions of these dimers, both the SRR's diameters and the spacing between them, may be comparable to the wavelength of the radiation. In those geometries, the required phase difference between resonators is achieved mainly through retardation. Thus, a smaller coupling strength is needed [20] to satisfy the condition for superdirectivity (Eq. 1). Hence, this allows the use of geometries such as those proposed in Ref. [24,25] using a planar configuration of SRRs in the same orientation ("CC"). This allows one to obtain the superdirective behavior with directivity $D = 4.6$. However, this value is still significantly smaller than the theoretically predicted one, as the size of the structure in the radiation direction is 0.25λ or larger. This provides noticeable retardation between the edges of the structure that, according to Ref. [4], must be neglectable to obtain the maximum possible directivity.

Nevertheless, the size of such elements inhibits the potential for further miniaturization, and, as the size of the structure becomes closer to the wavelength, the maximum theoretical possible directivity also drops. One way to overcome this limit is to reduce the resonance frequency of a split ring by soldering a capacitor into the gap [20,21]. Despite a close to theoretical maximum value of directivity, this approach has certain limitations because, to scale this up to 1 GHz, the diameter of the SRRs should be about 2 mm with capacitors soldered into a 0.02 mm gap; this presents a challenge in terms of sample manufacture.

Here, we propose improving the size-to-wavelength ratio at GHz frequencies with the use of helices instead of SRRs, as helices can act as a massively subwavelength resonator, while keeping the same high value of directivity. Furthermore, they can be easily scaled to operate at different frequencies and their quality factor can be controlled by changing the axial pitch, which provides further tuning opportunities.

III. METHODS

A. Experimental setup

The experimental setup of the superdirective dimer of helices is presented in Fig. 1. The helices are supported on a three-dimensionally printed platform of Ultimaker

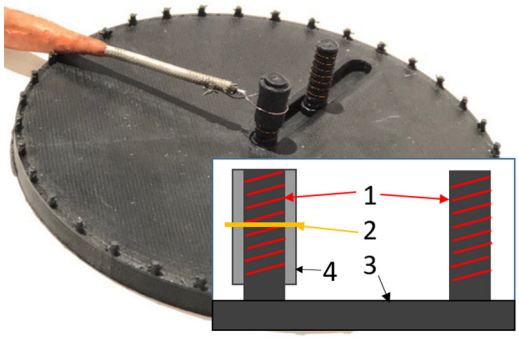

FIG. 1. Experimental setup of the superdirective dimer. Copper helices are wrapped around a polylactide (PLA) base ($\varepsilon = 2.6 + 0.04i$). Schematic of this structure is shown on the inset: 1, helices; 2, inductive loop; 3, dielectric base; 4, dielectric cover of the first element. Resonant frequency $f_0 = 1.534$ GHz; geometric parameters are as stated in Table I.

TABLE I. Parameters of helices.

	First element	Second element
n	7	7.6
H (mm)	8.75	9.5
R (mm)	2	2

black polylactide (PLA) ($\varepsilon = 2.6 + 0.04i$). The base is constructed so that the distance between the element centers can be freely changed from $a = 3$ to 35 mm, allowing one to readily satisfy the superdirective condition (Eq. 1). This base is fixed underneath the first helix to ensure precise rotation of the dimer in the experimental directivity measurements. We fabricate helices using copper wire with a wire radius of $r = 0.1$ mm. The parameters of the helices are listed in Table I.

Here, H is the height of elements, R is the major radius, and n is the number of turns. A schematic representation of the helices is presented in Fig. 2. The proximity of the feeding loop perturbs the resonant frequency of the first helix, and so we adjust the number of turns and height of the second helix (shown in Table I), so that their frequencies are matched ($f_0 = 1.54$ GHz).

The first helix is fed inductively via a concentrically placed single copper loop soldered to a semirigid coax cable. As the loop itself has a much higher resonant frequency than that of the helix, it does not radiate much power at the operational frequency, and thus, does not interfere with the far-field pattern of the dimer. However, the helical resonator geometry makes it possible to achieve high power transfer from the loop to the first helix. If only one helix is being fed, 98% of power is transferred at the resonance frequency (Fig. 3). However, when the second helix is introduced, the splitting of the resonant curve that

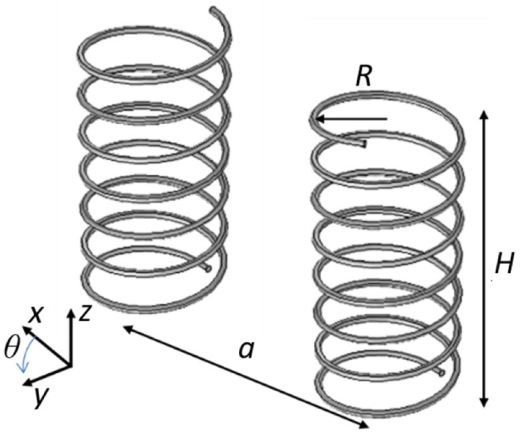

FIG. 2. Schematic representation of the helices. H, height; R, radius; a, distance between helix centers.

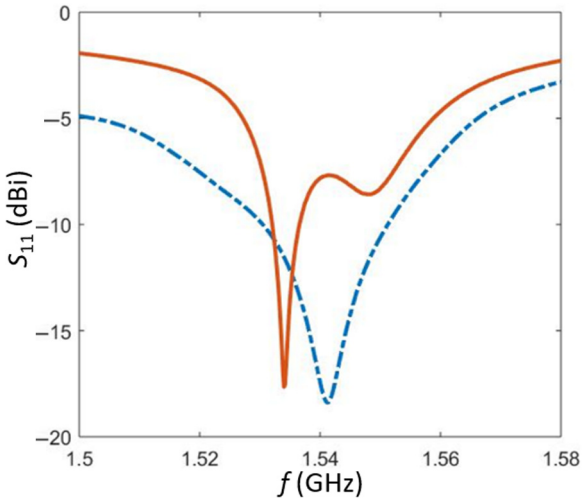

FIG. 3. Frequency dependence of the S_{11} parameter for the single helix (blue) and superdirective dimer (red).

is shown on Fig. 3 can be observed. The maximum directivity is obtained just below the lowest resonance of the structure, where 78% of power transfer can be obtained.

This value is determined experimentally from the S_{11} parameter, which suggests almost complete overlap of magnetic flux between the loop and the helix. The frequency dependence of the power transfer is presented on Fig. 4. The maximum power transfer is obtained at the lowest resonance of the structure (1.534 GHz), and the operational band of the dimer (marked with dashed lines) is just below that frequency. In addition, COMSOL modeling with assumed 100% coupling in efficiency gives a radiation efficiency of 82% for copper helices and a 45% efficiency for the steel helices discussed in Sec. V. (This difference in efficiency is due to greater Joule heating in steel, compared with that in copper.) Hence, the resulting radiation efficiency of the presented copper structure is estimated to be 64%. Radiation efficiency of 62% at the frequency of maximum directivity is obtained experimentally using a dipole antenna with a MACOM TP-101 balun providing 0.5 dB gain at its resonant frequency (1.534 GHz). Numerical and experimental results for efficiency are in a good agreement.

The experimental setup for far-field measurements is presented on Fig. 5. It is undertaken at 1 m distance from the dimer using a half-wavelength dipole antenna with 1.5 GHz resonant frequency. Data for the electric fields are obtained using a 40 GHz vector network analyzer (Anritsu MS4644A) and unwanted reflections and noise are suppressed by using a microwave foam absorber (ECCOSORB AN-77). Measurements are undertaken in the azimuth plane and then extrapolated to the whole 4π space by using analytical calculations from Ref. [17].

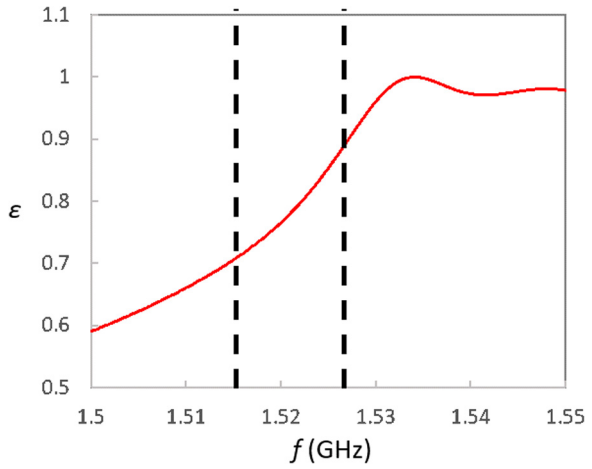

FIG. 4. Frequency dependence of the relative power transfer, ε, from the inductive loop to the first helix. Dashed lines mark the operational band of the dimer.

B. Numeric modeling

Numerical modeling of this work is undertaken using the finite element method (FEM) software COMSOL Multiphysics frequency domain solver. The geometry of the elements and permittivity of the dielectric base are chosen to match the experimental ones, so that the resonant frequency of each element is 1.54 GHz. The first element is fed using a single copper loop driven by a lumped port. The materials used are copper and stainless steel.

C. Analytical model

The analytical calculation of the directivity patterns of the superdirective dimers is based on two major parts. First, is the calculation of the dipole array directivity, as developed over the last century; a recent version of this calculation was reported by Shamonina and Solymar [16]. It uses the assumption that each element of the array is much smaller than the free-space wavelength and its radiation

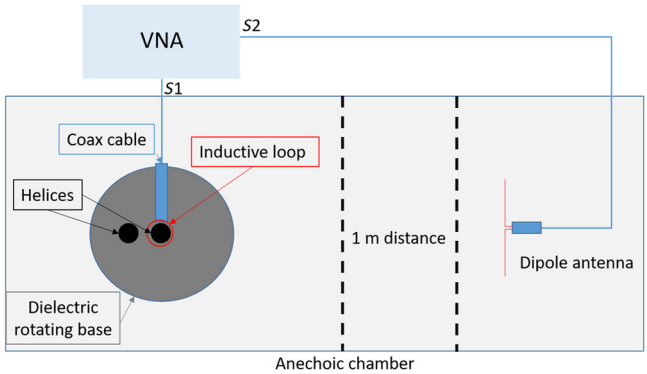

FIG. 5. Schematic representation of the far-field measurement experimental setup.

is dipolelike. By taking into account the current distribution across the array, the mutual arrangement of the dipoles and retardation of the electromagnetic waves, it allows one to obtain the far-field directivity patterns for the examined structure. The current (I) condition for superdirectivity in this case is

$$\frac{I_2}{I_1} = -1 - i\frac{2}{5}ka + \frac{2}{25}(ka)^2 + \ldots, \tag{2}$$

where the subscript on the current terms label the helix elements. Equation (2) effectively states that the currents in both the driven (1) and the magnetically coupled (2) elements should be equal in amplitude, but should almost be in antiphase for $ka \ll 1$. This situation pertains at the lowest resonance of the two negatively coupled resonators structure.

Second, to obtain useful analytical results, we calculate the current distributions in the array of two magnetically coupled elements, when one of them is driven and the other is passive. In this case, the LCR circuit model introduced in research on interelement coupling [18] may be used. The frequency dependence of currents I_1 and I_2 in the first and second elements of the dimer, respectively, may be expressed as

$$\begin{aligned} II_1 &= \frac{iV_0Z_0}{(Z_0^2 - Z_m^2)} \\ I_2 &= \frac{iV_0Z_m}{(Z_0^2 - Z_m^2)} \\ Z_0 &= i\omega L\left(1 - \frac{\omega_0^2}{\omega^2} + \frac{i\omega_0}{Q\omega}\right)^2, \\ Z_m &= i\omega M \end{aligned} \tag{3}$$

where V_0 is the excitation of the first element; ω_0 is the resonant frequency of the elements; L is their self-inductance; Q is the quality factor; and M is the mutual inductance, which is negative in the present cases. Values of V_0, Q, and f_0 can be obtained experimentally. M and the value of the coupling ($\kappa = 2M/L$) can be obtained using the coupling retrieval method described in Ref. [26], and L can be calculated from geometric parameters. At these frequencies, the common assumption of a purely real value of the coupling coefficient cannot be used, as retardation effects have a significant influence on the frequency dependence of currents in each of the elements. As a result, the coupling coefficient becomes complex and should be presented in the form $\kappa = |\kappa|e^{ika}$.

Currents obtained using Eq. (3) can then be used as input values for the dipole radiators in the model discussed above to obtain the frequency dependencies of directivity for any given set of parameters.

IV. DIMER OF HELICES

Experimental, analytical, and numerical data are obtained for the described configuration of helices. In Fig. 6, the experimental results are presented to illustrate the frequency dependence of directivity for different distances between helices. A maximum directivity of $5.05 = 7.03$ dBi, which is close to the theoretical maximum, is measured at 1.521 GHz.

The operational bandwidth (calculated at the level of -3 dB) is 14 MHz, which is 1% of the resonant frequency. Figure 7 illustrates a comparison between the analytical, numerical, and experimental directivity data close to the frequency of directivity maximum. High uncertainties at low and high frequencies are associated with the very small magnitude of signals away from resonance. Although the analytical model agrees with experiment within uncertainty, the small systematic difference between experiment and the FEM numerical model is likely to be because it is based on the *LCR* circuit model and does not take into account the frequency response associated with the dielectric base. The frequency dependence of the gain in this case is demonstrated in Fig. 8 for both experimental and numerical results. The maximum gain for this structure is $G = 3.13 = 4.95$ dB, which is close to the value predicted by COMSOL ($3.23 = 5.09$ dBi).

By increasing the distance between the elements, we also decrease the coupling between them, which results in a narrowing of the operational band. In contrast, for smaller distances and stronger coupling, the operational band widens and reaches 20 MHz for 12 mm separation. However, the maximum of the directivity for this case, $D_{\max} = 4.32 = 6.35$ dBi at 5.1 GHz, is significantly smaller than that for the optimal configuration. The dependence of the maximum directivity on the distance between the elements for both numerical and experimental results is shown in Fig. 9. This also agrees with a similar dependence presented in Ref. [16] for elements with resonant frequency in the MHz range.

The frequency corresponding to the maximum directivity is also affected by the coupling coefficient. As shown in Ref. [9], the coupling between resonators leads to two resonant frequencies, corresponding to in-phase and antiphase modes. In our case, the phase conditions for superdirectivity are met near the lower-frequency antiphase resonance

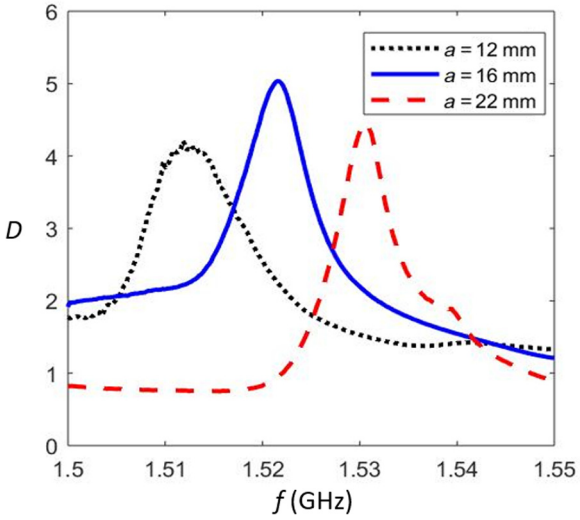

FIG. 6. Experimental results for the frequency dependence of the directivity for $a = 12$, 16, and 22 mm between helices.

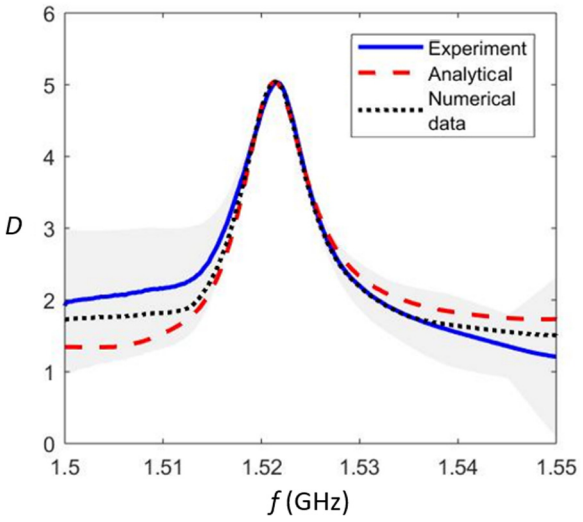

FIG. 7. Analytical, numerical, and experimental frequency dependencies of directivity for the superdirective dimer with $a = 16$ mm. Uncertainties for the experimental value are marked in light gray.

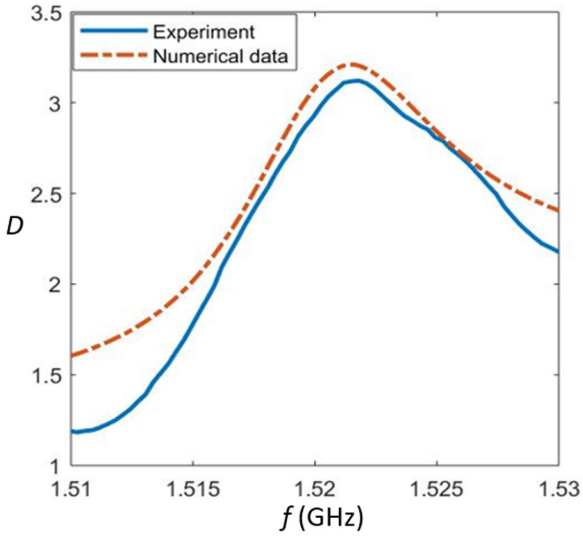

FIG. 8. Frequency dependence of the effective gain of the superdirective dimer in optimal configuration near the frequency of maximum directivity.

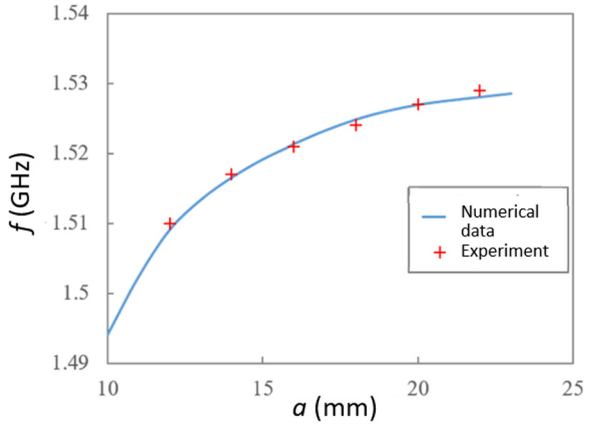

FIG. 9. Analytical and numerical results for maximum directivity dependence on the size of the superdirective dimer.

of the system. As the coupling becomes stronger and the antiphase resonance reduces in frequency, the maximum directivity is also achieved at corresponding lower frequencies. On the other hand, for weak coupling, the maximum directivity is achieved close to the resonant frequency of the single helix. This also agrees with numerical calculations, as shown in Fig. 10.

The directivity patterns for the optimum configuration at $f = 1.515$, 1.521, and 1.527 GHz are presented in Fig. 11. At low frequencies, power is radiated equally in both forward and backward directions. At the maximum directivity frequency, as predicted analytically, most power is radiated in the backward direction, while, for all other directions, radiation is suppressed through destructive interference. For higher frequencies, the angular width of the backward lobe grows, leading to a decrease in directivity. Good agreement between analytical, numerical, and experimental data is also observed here for all frequencies.

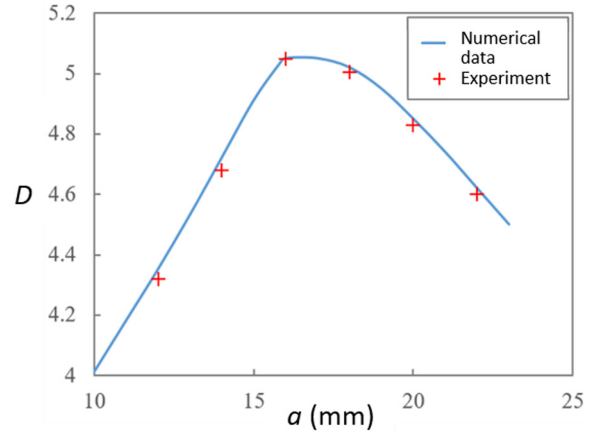

FIG. 10. Analytical and numerical results for the frequency of maximum directivity dependence on the size of the superdirective dimer.

The size of the optimized structure is 0.09λ in the radiation direction, 0.02λ wide, and 0.05λ high. These dimensions are smaller than the size of previously the proposed SRR dimer on the printed circuit board ($0.25 \times 0.122 \times 0.007\lambda^3$) and even the diameter of one SRR (0.12λ) [26]. Although the height of the SRR is minimized, we still achieve more than 2 times reduction in the resulting volume.

With this optimized structure close to the theoretical maximum, values of directivity are experimentally achieved for the simple structure of two coupled resonators, each of which provides dipolelike radiation.

V. FURTHER OPTIMIZATION PROSPECTS

Our geometry is demonstrated to provide the highest experimentally realized value of superdirective dimer directivity, via an antenna system that is compact, efficient, and easy to make. However, there are further potential benefits of using helical elements, since they provide some new degrees of freedom that offer increased functionality.

There are several parameters that can be varied in helices: height, number of turns, axial pitch, radius, wire thickness, and helical handedness. However, in terms of directivity of the dimer, it is important to control the resonant frequency, quality factor, and coupling between helices. All spatial parameters affect all three of these parameters, to some extent, and can be tuned to satisfy the superdirective condition, as long as the structure stays subwavelength in all directions. As for handedness, this does not affect the quality factor or the resonant frequency of the helices, and, as we work at the main (dipolelike) mode of helical radiation, there is no chirality in the behavior of our structure. Thus, different handedness affects only the coupling coefficient by increasing its electric component, which leads to a greater distance being required to satisfy the superdirective condition: 19 mm for different-handed helices, compared with 16 mm for the same-handed ones.

The structure described above already provides close to maximum value of directivity, but further optimization may be done to reduce the size of the structure. According to Eq. (1), we may reduce the quality factor or coupling between elements without affecting the resonant frequencies. However, κ grows rapidly for decreasing distances, and thus, the only option is to vary the quality factor of the resonant elements themselves. Conventionally, Q can be controlled by using lower conductivity metals; however, as stated before, helices also provide an opportunity to tune their Q factor by varying the geometric parameters of helices that change both their self-inductance and self-capacitance. The parameter that is the most suitable in this case is the height of the helices, as it provides significant control over the Q factor, while having just a minor influence on resonant frequency or coupling. For instance, the helices presented above with $H = 10$ mm have $Q = 98$. For

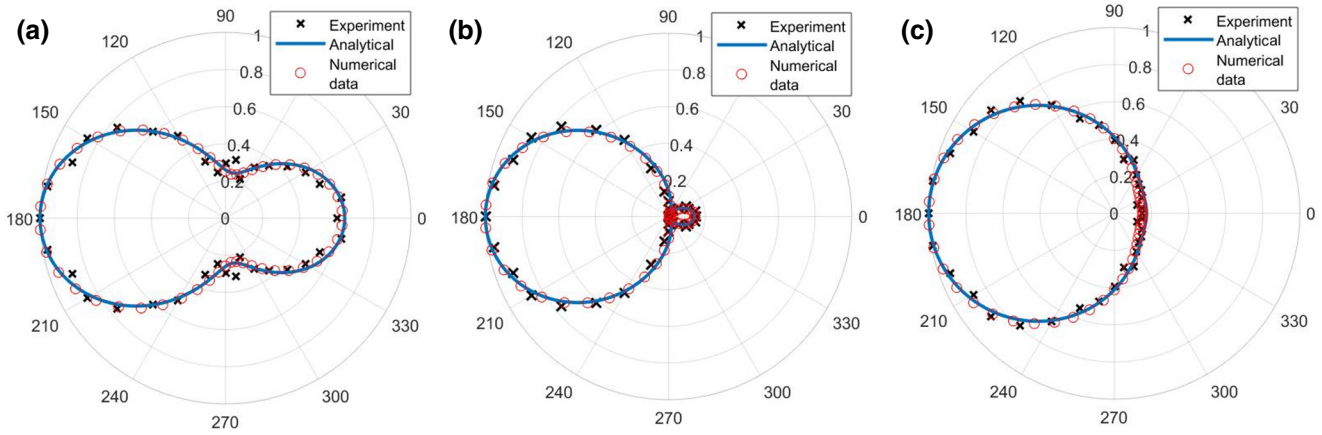

FIG. 11. Analytical, numerical, and experimental directivity patterns for the superdirective dimer with $a = 16$ mm. (a) $f = 1.515$ GHz, (b) $f = 1.521$ GHz, (c) $f = 1.527$ GHz.

helices with the same wire length and $H = 5$ mm, $Q = 157$, while, for $H = 20$ mm, $Q = 62$. By combining these two approaches, it is possible to significantly improve the antenna performance.

For instance, steel helices, with substantially reduced conductivity, with $H = 20$ mm, $Q = 21$ arranged at $a = 10$ mm distance, are shown to provide a directivity of $D = 5.15 = 7.12$ dBi, which is closer to the theoretical maximum due to the smaller size of the structure in the azimuth plane. Analytical and numerical results for the frequency dependence of directivity in this case are presented in Fig. 12. The resonance frequency is shifted to 1.71 GHz because of the decrease in self-inductance and capacitance of the helices. Moreover, as coupling for such a structure is stronger than that in the one presented above, the operational bandwidth of the dimer reaches 81 MHz; this is a factor of four increase compared with that of the copper ones.

The dependence of the optimal dimer size on the Q factor of individual helices for $H = 10$ mm is demonstrated in Fig. 13. The size could be greatly reduced using less-conductive materials. (The main limitation here is that the superdirective condition becomes disturbed when the distance between elements is comparable with that of their diameter.)

However, there is a significant drawback associated with these benefits due to the increasing losses arising from Joule heating. In the example above, a 3 times reduction in the Q factor lowers the radiation efficiency to about 35% and the dependence of the resulting gain on the Q factor is presented in Fig. 14. It can be seen that the gain drops significantly below two for the least conductive elements, while, for the structures with conductivity beyond that of copper, the gain saturates at a level of about 3.7.

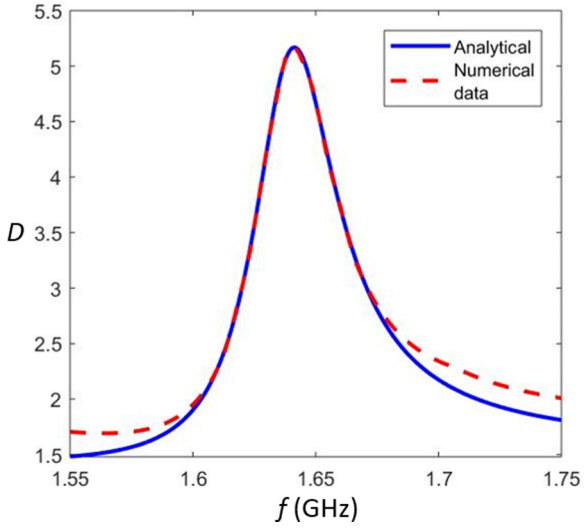

FIG. 12. Analytical dependencies of superdirectivity for the steel dimer with $a = 10$ mm, $f_0 = 1.71$ GHz.

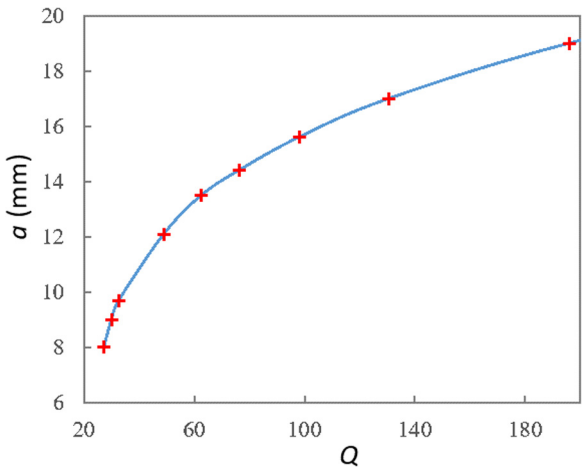

FIG. 13. Numerical results for the dependence of the optimal dimer size on the Q factor of individual helices for $H = 10$ mm.

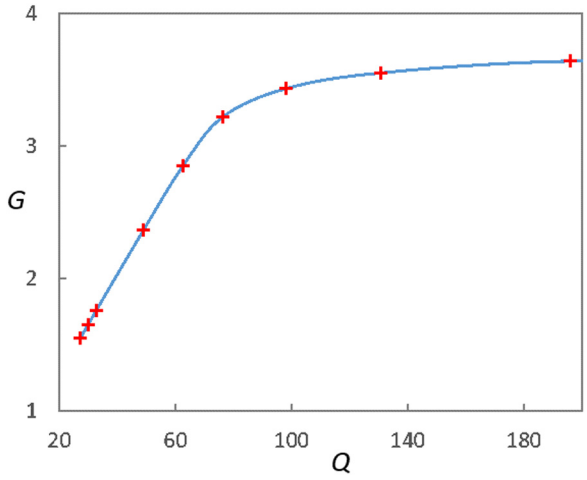

FIG. 14. Numerical results for the dependence of the superdirective dimer gain on the Q factor of individual helices for $H = 10$ mm.

VI. CONCLUSIONS

Superdirective dimers of dipolelike resonators with directivity values of $D > 5 = 7$ dBi are experimentally demonstrated in the low-GHz frequency range. The helical geometry, while being simple to make, provides more than a 3 times reduction in size and permits the use of strong power transfer from an inductive loop of 78%. Numerical and analytical results are in good agreement with experimental data. The radiation properties of this structure are studied as a function of the distance between the elements. Ways of optimizing the directivity, efficiency, size, and operational passband are demonstrated. The presented results prove the possibility of reaching close to the theoretical maximum directivity values and provide a basis to construct superdirective arrays with larger numbers of elements.

Although the structure described here is made manually, helical dipoles such as this can be manufactured using double-sided printed circuit boards. Such a method has already been used to create helical structures [27].

Such antennas can be applied for interference-limited systems, such as WLAN access points or other small-cell applications, where high directivity and small size are required.

All data created during this research are openly available from the University of Exeter's institutional repository [28].

ACKNOWLEDGMENT

We acknowledge financial support from the Engineering and Physical Sciences Research Council (EPSRC) of the United Kingdom via the EPSRC Centre for Doctoral Training in Metamaterials (Grant No. EP/L015331/1). We also acknowledge financial support from the Defence Science and Technology Laboratory (Dstl), (Contract No: DSTLX1000133579).

[1] W. Oseen, Die einsteinsche nadelstichstrahlung und die maxwellschen gleichungen, Ann. D. Phys. **69**, 202204 (1922).
[2] A. Schelkunoff, A mathematical theory of linear arrays, Bell Syst. Tech. J. **22**, 80107 (1943).
[3] A. Uzkov, An approach to the problem of optimum directive antenna design, Compt. Rend. Dokl. Acad. Sci. USSR **53**, 3538 (1946).
[4] M. Uzsoky and L. Solymar, Theory of superdirective linear arrays, Acta Physica Acad. Hung. Sci. **6**, 185205 (1956).
[5] L. Solymar, Maximum gain of a line source antenna if the distribution function is a finite Fourier series, IRE Trans. Antennas Propag **6**, 215219 (1958).
[6] K. Itoh, K. ltoh, O. lshii, Y. Nagai, N. Suzuki, Y. Kimachi, and O. Michikami, Two-element superdirective array antenna composed of high-T c superconducting small helical radiators, J. Supercond. **5**, 485490 (1992).
[7] J. Bacon and R. Medhurst, Superdirective aerial array containing only one fed element, Proc. IEE **116**, 365372 (1969).
[8] G. Andrasic and J. R. James, Height reduced superdirective array with helical directors, Electron. Lett. **29**, 20022004 (1993).
[9] E. Shamonina, A. Kalinin, H. Ringhofer, and L. Solymar, Magnetoinductive waves in one, two, and three dimensions, J. Appl. Phys. **92**, 62526261 (2002).
[10] L. Solymar and E. Shamonina, *Waves in Metamaterials* (Oxford University Press, Oxford, 2009).
[11] K. Buell, H. Mosallaei, and K. Sarabandi, Metamaterial insulator enabled superdirective array, IEEE Trans. Antennas Propag. **55**, 10741085 (2005).
[12] A. Yaghjian, T. O'Donnell, E. Altshuler, and S. Best, Electrically small supergain end-fire arrays, Radio Sci. **43**, 3002113 (2008).
[13] T. O'Donnell and A. Yaghjian, in Proc. IEEE Antennas Propag. Soc. Int. Symp. (2006), pp. 31113114.
[14] S. Lim and H. Ling, Design of electrically small, pattern reconfigurable yagi antenna, Electron. Lett. **43**, 24 (2007).
[15] E. Shamonina and L. Solymar, in IEEE Proc. 7th Int. Congress on Advanced Electromagnetic Materials in Microwaves and Optics (Metamaterials 2013) (2013), pp. 9799.
[16] E. Shamonina and L. Solymar, in IEEE Proc. 8th Int. Congress on Advanced Electromagnetic Materials in Microwaves and Optics (Metamaterials 2014) (2014), pp. 268279.
[17] E. Shamonina and L. Solymar, Maximum directivity of arbitrary dipole arrays, IET Microw. Antennas Propag. **9**, 101107 (2014).
[18] E. E. Altshuler, T. H. O'Donnell, A. D. Yaghjian, and S. R. Best, A monopole superdirective array, IEEE Trans. Antennas Propag. **53**, 26532661 (2005).

[19] E. Tatartschuk, N. Gneiding, F. Hesmer, A. Radkovskaya, and E. Shamonina, Mapping inter-element coupling in metamaterials: Scaling down to infrared, J. Appl. Phys. **111**, 09490419 (2012).

[20] P. Petrov, A. Radkovskaya, C. J. Stevens, and E. Shamonina, in IEEE Proc. 11th Int. Congress on Engineered Materials Platforms for Novel Wave Phenomena (2017), pp. 265267.

[21] A. Radkovskaya, S. Kiriushechkina, A. Vakulenko, P. Petrov, L. Solymar, L. Li, A. Vallecchi, C. J. Stevens, and E. Shamonina, Superdirectivity from arrays of strongly coupled meta-atoms, J. Appl. Phys. **124**, 104901 (2018).

[22] T. Kokkinos and A. P. Feresidis, Electrically small superdirective endfire arrays of metamaterial-inspired Low-profile monopoles, IEEE Antennas Wirel. Propag. Lett. **11**, 568571 (2012).

[23] J. Diao and K. F. Warnick, Practical superdirectivity With resonant screened apertures motivated by a poynting streamlines analysis, IEEE Trans. Antennas Propag. **66**, 432437 (2017).

[24] A. Radkovskaya, A. Vallecchi, L. Li, G. Faulkner, C. Stevens, and E. Shamonina, in Proc. 10th Int. Cong. On Advanced Electromagnetic Metamaterials in Microwaves and Optics (2016), pp. 283285.

[25] J. Yan, A. Radkovskaya, A. Vallecchi, C. Stevens, and E. Shamonina, in Proc. 12th European Conference on Antennas and Propagation (EuCAP 2018) (2018), pp. 295300.

[26] P. Petrov, A. Radkovskaya, and E. Shamonina, in IEEE Proc. 9th Int. Cong. On Advanced Electromagnetic Metamaterials in Microwaves and Optics (2015), pp. 259261.

[27] B. Yang, Q. Guo, B. Tremain, L. E. Barr, W. Gao, H. Liu, B. Béri, Y. Xiang, D. Fan, A. P. Hibbins, and S. Zhang, Direct observation of topological surface-state arcs in photonic metamaterials, Nat. Commun. **8**, 97 (2017).

[28] P. Petrov, A. P. Hibbins, and J. R. Sambles, Data for: "Microwave superdirectivity with dimers of helical elements," University of Exeter, https://ore.exeter.ac.uk/ (2020).